Single-cell immune profiling of atherosclerosis: from omics to therapeutics

Depuydt, M.A.C.

Chapter 6

Aging promotes mast cell activation and antigen presenting capacity in atherosclerosis

Manuscript in preparation

Marie A.C. Depuydt*[1], Virginia Smit*[1], Frank H. Schaftenaar[1], Esmeralda Hemme[1], Lucie Delfos[1], Femke Vlaswinkel[1], Conor Simpson[1], Petri T. Kovanen[2], Bram Slütter[1], Johan Kuiper, Ilze Bot#, Amanda C. Foks#

1 Division of BioTherapeutics, Leiden Academic Centre for Drug Research, Leiden University, 2333 CC, Leiden, The Netherlands
2 Wihuri Research Institute, Helsinki, Finland.

*These authors contributed equally; #Shared last authors.

Abstract

Aging is an independent and dominant risk factor for atherosclerosis and is associated with a low-grade chronic inflammation termed inflammaging. This age-induced pro-inflammatory environment may have great impact on plaque-residing immune cells, including mast cells. Mast cells have been found to accumulate in the human atherosclerotic plaque upon disease progression and have been associated with plaque instability. However, it is currently unknown whether aging drives the pro-atherogenic effects of mast cells in atherosclerosis.

To assess the effects of aging on mast cell phenotype, we examined mast cell populations in young and old male *Ldlr*$^{-/-}$ mice fed either a chow or Western-type diet. We found that in atherosclerotic tissue both mast cell number and activation status increased upon aging. Furthermore, we identified that aged bone-marrow derived mast cells displayed increased basal CD63 expression compared to young cells, indicative of intrinsic low-grade activation. Moreover, we demonstrated that aging increases the amount of MHCII^{+} mast cells in atherosclerosis, allowing them to act as antigen-presenting cells, which correspondingly led to increased CD4^{+} T cell proliferation *in vitro*. Finally, single-cell RNA sequencing of human atherosclerotic plaques confirmed mast cell-specific expression of MHC-II orthologs.

To conclude, we established that aging induces phenotypic changes of mast cells in atherosclerosis, regarding both activation status and antigen presenting capacity, which can contribute to disease progression.

Introduction

Acute cardiovascular syndromes are the principal cause of death in the Western society. The main pathology underlying the majority of cardiovascular diseases is atherosclerosis, which is caused by the accumulation of lipids and inflammatory cells in the vessel wall. Upon progression and destabilization of an atherosclerotic plaque, the risk of plaque rupture increases. Rupture or erosion of an atherosclerotic plaque can subsequently lead to vessel-occluding thrombosis, potentially resulting in acute cardiovascular syndromes such as myocardial infarction or stroke.[1]

The mast cell, a potent immune effector cell primarily involved in host defense responses[2,3], has been implicated in atherosclerotic plaque destabilization. Previously, we and others established that mast cells contribute to plaque development in experimental models of atherosclerosis[4,5]. Excessive mast cell activation resulted in an increased incidence of intraplaque hemorrhage, a hallmark of plaque instability in murine atherosclerosis[4]. Also in human atherosclerotic plaques, mast cell numbers increased upon plaque progression and were significantly elevated in plaques that contained an intraplaque hemorrhage[6]. Strikingly, mast cell numbers in advanced carotid artery plaques, obtained with carotid endarterectomy, were elevated in patients that suffered a clinical event during follow-up[6]. Together, these data suggest that mast cells actively contribute to atherosclerotic plaque progression and destabilization. Age is an important risk factor for atherosclerosis.[7] However, aging also leads to structural changes in immune responses with skewing towards myeloid at the cost of lymphoid lineages[8] and to an enduring state of low-grade inflammation (inflammaging), in which mast cells may participate as well. Few studies have investigated the effects of aging on mast cells.[9–11] In gut and brain for example, increasing numbers of mast cells were reported upon aging, which were implicated in prolonged inflammatory responses in a mouse model of stroke.[10] Also in human skin, mast cells accumulate upon aging, with altered functionality.[11] In these aged skin samples, a reduced gene expression of for example Substance P was observed compared to young, which has previously been described as potent mast cell activator via different receptors. This illustrates the importance of taking age into account upon therapeutic intervention. It is however unknown how aging impacts mast cells in atherosclerosis. Combined with the fact that mast cell numbers increase with disease progression, detailed mechanistic insights in age-associated changes in mast cell behavior is highly relevant in advanced atherosclerosis. In this study, we therefore aimed to assess the effects of aging on mast cell phenotype and activation status in atherosclerosis.

Methods

Animals

All animal experiments were performed in compliance with the guidelines of the Dutch government and the Directive 2010/63/EU of the European Parliament. The experiments were approved by the Ethics Committee for Animal Experiments and the Animal Welfare Body of Leiden University (Project 106002017887).

Aging cohort

Male young (10-12 weeks) and old (75-83 weeks) in-house bred *Ldlr*$^{-/-}$ mice on a C57BL/6 background (n = 8-9/group) were provided with food and water *ad libitum*. Young mice were either fed a regular chow diet or a Western-type diet (0.25% cholesterol, 15% cocoa butter, Special Diet Services, Essex, UK) for 5 weeks. Old mice were fed a regular chow diet. Mice were randomized based on weight and serum cholesterol levels. At week 5, mice were sacrificed upon subcutaneous injection of anaesthetics (ketamine (100 mg/kg), atropine (0.6 mg/kg) and xylazine (10 mg/kg)), followed by orbital bleeding, after which peritoneal lavage was performed with PBS. Next, mice were perfused with phosphate-buffered saline (PBS) through the left cardiac ventricle. Subsequently, organs were collected for analysis.

Adoptive transfer cohort

Male 15-22 week old *apoE*$^{-/-}$*Kit*$^{W\text{-}sh/W\text{-}sh}$ (n = 9-12/group) were provided with food and water *ad libitum*. Mice were randomized based on age, weight and serum cholesterol levels. At the start of the experiment, mice were injected intravenously with 10*10^{6} bone marrow-derived mast cells originating from either young or old *Ldlr*$^{-/-}$ mice and simultaneously put on a Western-type diet. After 14 weeks, mice were sacrificed as described above.

DSCG cohort

Male old (68-73 weeks) *Ldlr*$^{-/-}$ mice on a C57BL/6 background (n=13-14/group) were provided with food and water *ad libitum*. Mice were randomized based on age, weight and serum cholesterol levels and were fed a chow diet throughout the experiment. Mice were treated with disodium cromoglycate (DSCG; 50 mg/kg i.p.) or PBS control three times a week. After 6 weeks of treatment, mice were sacrificed as described above.

OT-II mice

OT-II mice were purchased from the Jackson Laboratory and further bred in house. Male 18 week old OT-II mice were sacrificed by cervical dislocation. Next, spleens were obtained for isolation of CD4^{+} T cells.

Histology

Hearts were dissected, embedded and frozen in Tissue-Tek OCT compound (Sakura). 10 µm cryosections of the aortic root were prepared for histological analysis. Mean plaque size and the percentage plaque area of total vessel area (vessel occlusion) were assessed by Oil-Red-O (ORO) staining. From the first appearance of the three aortic valves, 5 consecutive slides with 80 µm distance between the sections were analysed for total lesion size within the three valves, after which the average lesion size was calculated. Naphthol AS-D chloroacetate staining (Sigma-Aldrich) was performed to manually quantify resting and activated mast cells in the atherosclerotic aortic root. A mast cell was considered resting when all granula were maintained inside the cell, while mast cells were assessed as activated when granula were deposited in the tissue surrounding the mast cell. Collagen content of the plaque was measured using either a Sirius Red staining in the adoptive transfer study or a Masson's trichrome staining in the DSCG study. Similarly, the average necrotic core size was quantified by measuring the acellular debris-rich areas of the plaque of three sections per mouse. For all stainings, three sections per mouse were analysed and averaged unless stated otherwise. Sections were obtained using either a Leica DMRE microscope (Leica Systems) or digitalised using a Panoramic 250 Flash III slide scanner (3DHISTECH, Hungary). Blinded analysis was performed using ImageJ software.

Cell isolation

Blood samples were lysed with ACK lysis buffer (0.15 M NH_4Cl, 1 mM $KHCO_3$, 0.1 mM Na_2EDTA, pH 7.3) to obtain a single white blood cell suspension. Spleens were passed through a 70 µm cell strainer (Greiner, Bio-one, Kremsmunster, Austria) and splenocytes were subsequently lysed with ACK lysis buffer. Aortic arches were cut into small pieces and enzymatically digested in a digestion mix containing collagenase I (450 U/mL), collagenase XI (250 U/mL), DNAse (120 U/mL), and hyaluronidase (120 U/mL; all Sigma-Aldrich) for 30 minutes at 37°C while shaking. After incubation, all samples were passed through a 70 µm cell strainer (Geiner, Bio-one, Kremsmunster, Austria). Single cell suspensions were then used for flow cytometry analysis.

Flow cytometry

Single cell suspensions from the aortic arch, peritoneum, blood and spleen were extracellularly stained with a mixture of selected fluorescent labelled antibodies for 30 minutes at 4°C. For intracellular stainings, cells were fixed and permeabilized with the Foxp3 Transcription Factor Staining buffer set (ThermoFisher) according to the manufacturer's protocol and stained with intracellular antibodies for 30

minutes at 4°C.The antibodies used for flow cytometry are listed in **Table S1**. All measurements were performed on a Cytoflex S (Beckman and Coulter, USA) and analysed with FlowJo v10.7 (Treestar, San Carlos, CA, USA).

Serum IgE measurement

Serum was collected through centrifugation at 8000 rpm for 10 minutes at 4°C and stored at -80°C until further use. IgE was measured using an IgE ELISA kit (Biolegend) according to manufacturer's instructions.

Bone-marrow derived mast cell culture

To obtain bone marrow-derived mast cells (BMMCs), bone marrow cells from young and old *Ldlr*$^{-/-}$ mice were cultured in RPMI 1640 containing 25 mM HEPES (Lonza) and supplemented with 10% fetal calf serum, 1% L-glutamine (Lonza), 100 U/mL mix of penicillin/streptomycin (PAA), 1% sodium pyruvate (Sigma-Aldrich), 1% non-essential amino acids (MEM NEAA; Gibco) and 5 ng/mL IL-3 (Immunotools). Cells were incubated at 37°C and 5% CO_2 and were kept at a density of 0.25*10^6 cells per mL by weekly subculturing. BMMCs were cultured for 4 weeks in total to obtain mature mast cells.

In vitro mast cell stimulation

The mast cell activation assay was performed using 1*10^6 young or old BMMCs. All mast cells were first sensitized with anti-DNP IgE (1µg/mL, Sigma-Aldrich) for 2.5 hours at 37°C and 5% CO_2. Subsequently, DNP-HSA (20 ng/mL, Sigma-Aldrich) or medium control was added for 30 min at 37°C and 5% CO_2 to obtain respectively stimulated and unstimulated mast cells. Mast cell activation was measured as percentage CD63$^+$ of live CD117$^+$FcεRI$^+$ mast cells. Cytokines in the supernatant were measured using a Legendplex assay (Biolegend), which was performed according to the manufacturers protocol.

Mast cell – OT-II CD4$^+$ T cell co-culture

Young and old BMMCs were cultured as described above. To induce MHC-II expression, mast cells were stimulated with IFN-γ (50 ng/mL) and IL-4 (20 ng/mL) for 48 hours. After 24 hours the medium was supplemented with new cytokines. MHC-II expression was measured as percentage MHC-II$^+$ of live CD117$^+$FcεRI$^+$ cells. CD4$^+$ T cells from OT-II mice were obtained using magnetic bead isolation by negative selection (Miltenyi Biotec) and stained with CFSE for 10 minutes at 37°C and 5% CO_2. Subsequently, the CD4$^+$ T cells were stimulated with anti-CD3 (1 µg/mL) and anti-CD28 (0.5 µg/mL) for 24 hours. Next, cells were washed and the OT-II CD4$^+$ T cells were seeded with the MHC-II$^+$ mast cells in a 1:1 ratio. Finally, 1 µg/mL

ovalbumin (OVA) was added to the co-cultured cells for 48 hours. All cells in this experiment were cultured in RPMI supplemented with 10% Fetal Bovine Serum, 1% Penicillin and Streptomycin, 1% L-glutamine and 0.05mM 2-mercaptoethanol. Subsequently, $CD4^+$ T cell proliferation was assessed by flow cytometry as the $\%CFSE^-$ of live $CD4^+$ T cells.

Single-cell RNA sequencing of human atherosclerotic plaques

Human carotid artery plaques were collected from 46 patients (26 male, 20 female) that underwent carotid endarterectomy surgery as part of AtheroExpress, an ongoing biobank study at the University Medical Centre Utrecht (Study approval number TME/C-01.18, protocol number 03/114).[12] Single cells were obtained and processed for single-cell RNA sequencing as previously described.[13] All studies were performed in accordance with the Declaration of Helsinki. Informed consent was obtained from all subjects involved in the study.

Statistical analysis

All data are represented as mean ± SEM and analysed in GraphPad Prism 9. Shapiro-Wilkson normality test was used to test data for normal distribution. In the aging cohort, statistical analysis was performed using one-way ANOVA or, if not normal distributed data, a Kruskal-Wallis test. For both the adoptive transfer study and the DSCG study, an unpaired two-tailed Student *t*-test or, in case of not normally distributed data, Mann-Whitney test was used. $P < 0.05$ was considered to be significant.

Results

Increased number of activated mast cells in the aged atherosclerotic aorta

Multiple age-related changes in mast cells have been described so far. Mast cells have been reported to accumulate in the skin, gut and brain with aging, however changes in mast cell activation differ per tissue.[10,11,14,15] Here, we first examined whether increased age affects mast cell numbers and activation status in the atherosclerotic environment. To this extent, we assessed mast cell phenotype in young male *Ldlr*$^{-/-}$ mice on either a chow (non-atherosclerotic, CD) or Western type diet (5 weeks, atherosclerotic, WD) and aged male *Ldlr*$^{-/-}$ mice on a CD that gradually developed atherosclerosis over time (**Fig. 1a**).[16]

Using flow cytometry, we observed a strong 6-fold increase in the total number of $CD117^+$ $Fc\varepsilon RI^+$ mast cells in the aortic arch of aged *Ldlr*$^{-/-}$ mice compared to young CD- and WD-fed *Ldlr*$^{-/-}$ mice (YC: 4.5±0.7, YW: 45.3±15.2, OC: 279.4±9 cells per aorta, YC vs.

OC $p<0.01$, YW vs. OC $p<0.01$; **Fig. 1b, c, Supplemental Fig. 1**). Additionally, a significant increase in mast cells as percentage of live CD45$^+$ immune cells was detected both in the aged atherosclerotic aorta and in the aged peritoneum (**Fig. 1d, e**).

To examine whether age also affects mast cell activation status, we measured CD63$^+$ expression, which is a marker that is upregulated upon mast cell degranulation.[17] In the aortic arch, a significant increase in the absolute number of CD63$^+$ mast cells was detected in the aged group compared to both young groups (YC: 1.8±0.6, YW: 41.3±13.6, OC: 259.7±85.4 per aorta, YC vs. OC $p<0.01$, YW vs. OC $p<0.01$; **Fig. 1f**). Correspondingly, an increased percentage of CD63$^+$ mast cells of live CD45$^+$ was observed in both young and old atherosclerotic aortas compared to young non-atherosclerotic aorta's (**Fig. 1g**). Of note, the difference in mast cell activation between young WD-fed and old *Ldlr*$^{-/-}$ mice is mainly attributed to the amount of mast cells and not the level of CD63 expression (**Supplemental Fig. 2a**). Similar to the aortic arch the percentage of CD63$^+$ peritoneal mast cells was significantly increased in aged mice as compared to young, indicating that overall the proportion of activated mast cells in a model of aged atherosclerosis is augmented (**Fig. 1h**). Subsequently, we histologically assessed mast cell quantity and activation status in the aortic root. While we did not observe a difference in the number of adventitial mast cells between the groups (**Fig. 1i, j**), the percentage of activated (degranulated) mast cells was increased in the adventitia of aged *Ldlr*$^{-/-}$ mice compared to both young counterparts (YC: 49±3, YW: 45±3, OC: 63±2, YC vs. OC $p<0.001$, YW vs. OC $p<0.01$; **Fig. 1i, k**).

As the Immunoglobulin E (IgE)-FcεRI pathway is the most commonly known mast cell activation pathway[18], we measured circulating total IgE levels. We observed significantly elevated IgE levels in serum of aged compared to young *Ldlr*$^{-/-}$ mice (YC: 44.1±9.9 ng/mL, YW: 44.2±19.0 pg/mL, 163.4±32.0 pg/mL, YC vs. OC $p<0.05$, YW vs. OC $p<0.01$; **Fig. 1l**), supporting the possibility of enhanced IgE-mediated mast cell activation in the aorta.

We next examined whether aging also induced mast cell-intrinsic changes. No differences in maximal activation were observed between *in vitro* stimulated young and old BMMCs, however increased basal CD63 expression was observed on old BMMCs compared to young (Young: 0.14±0.006% vs. Old: 4.4±0.2%, $p<0.05$; **Fig. 1m, n**). Moreover, a significant increase of CC chemokine ligand 2 (CCL2) was observed in the supernatant of old stimulated BMMCs (Young: 198.5±5.4 pg/mL vs. Old: 238.0±11.8 pg/mL, $p<0.05$; **Fig. 1o**). No differences were observed for CCL3, CCL4, Interleukin (IL)-4, IL-6 and TNF-α (**Supplemental Fig 2b-f**). For unstimulated samples, all chemokines and cytokines measured had values below the detection limit.

Increased MHCII$^+$ expression on mast cells of old miceinduces vigorous CD4$^+$ T cell proliferation

Although mast cells are most commonly known for their pro-inflammatory secretome, there is accumulating evidence that they also act as atypical antigen presenting cells.[19] Therefore, we subsequently examined whether age affects Major Histocompatibility Complex (MHC)-II expression on mast cells. A respectively 63- and 4-fold increase in the number of MHC-II$^+$ mast cells was observed in aged compared to young CD-fed and WD-fed *Ldlr*$^{-/-}$ mice (YC: 2.5±0.5, YW: 40.8±14.7, OC: 157.7±40.5 per aorta, YC vs. OC $p<0.001$, YW vs. OC $p<0.01$; **Fig. 2a**). Similarly, the proportion of MHCII$^+$ mast cells accumulated was also significantly enlarged in the aged atherosclerotic aorta (YC: 0.1±0.03% vs OC: 3.0±0.6, $p<0.001$; **Fig. 2a**). This particular difference was also detected in peritoneal mast cells (**Fig. 2b**). Subsequently, we assessed whether aged mast cells have increased potential to induce CD4$^+$ T cell proliferation. We first stimulated BMMCs derived from both young and aged bone marrow with IFN-γ and IL-4 for two days to enhance MHCII expression as previously described.[20,21] A significant increase in MHC-II expression was detected on aged BMMCs versus young upon stimulation (**Fig. 2c**). Subsequently, co-culture of aged BMMCs with CD4$^+$ T cells resulted in significantly increased CD4$^+$ T cell proliferation (Young: 35.2±1.2% vs. Old: 45.8±1.2%, $p<0.001$ **Fig. 2d**). Finally, we examined expression of human MHC-II orthologs on mast cells detected in a single-cell RNA sequencing data set of 43 atherosclerotic plaques obtained by carotid endarterectomy surgery from aged patients. Expression of *HLA-DPA1*, *HLA-DRA* and *HLA-DRB1* was observed on the majority of the detected mast cells, suggesting that mast cells can act as antigen presenting cells in the human atherosclerotic plaque as well (**Fig. 2e**).

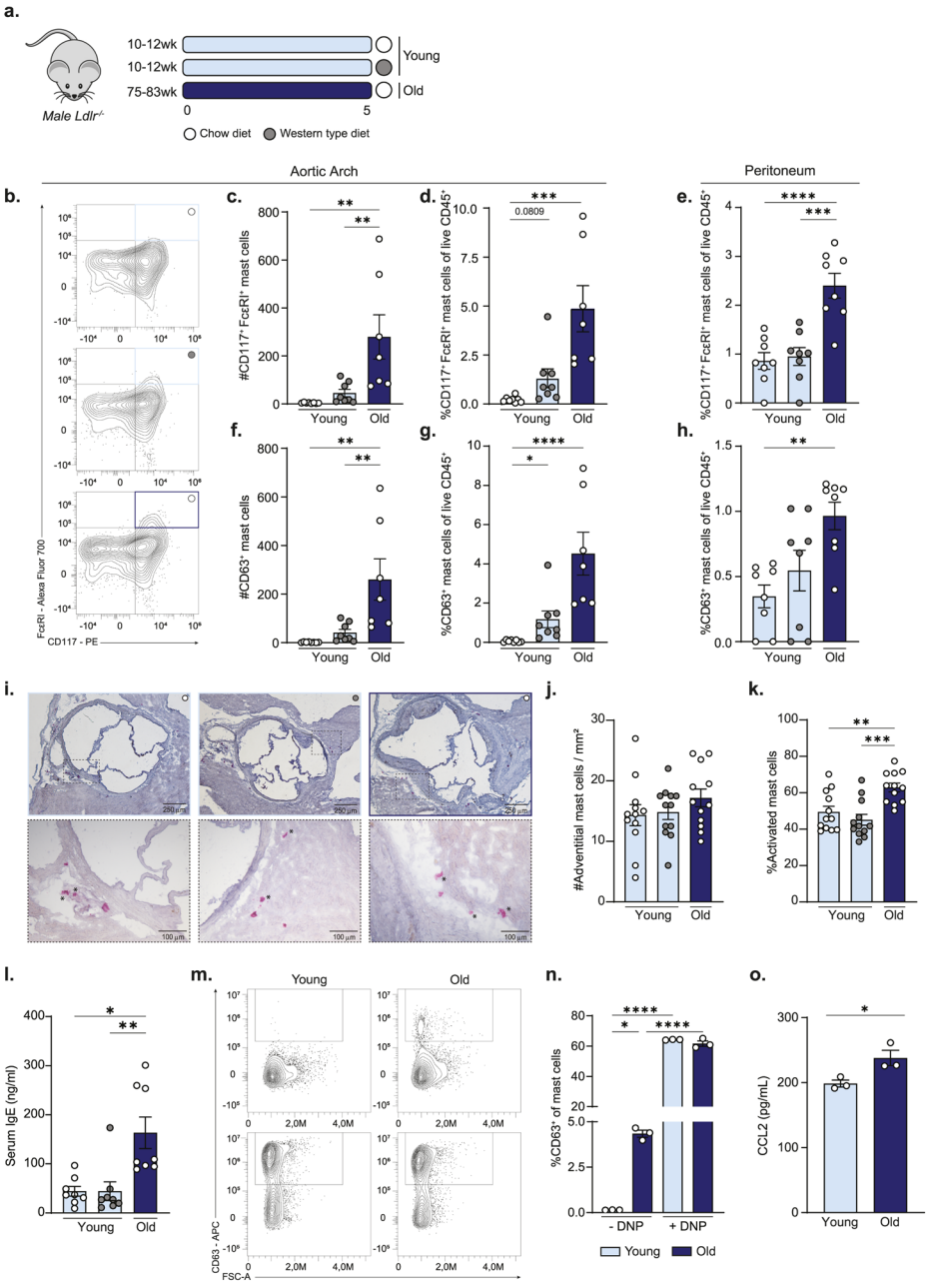
a.
Male Ldlr-/-
10-12wk
10-12wk
75-83wk
Young
Old
0
5
Chow diet
Western type diet
Aortic Arch
Peritoneum
b.
FcεRI - Alexa Fluor 700
CD117 - PE
c.
#CD117+ FcεRI+ mast cells
d.
%CD117+ FcεRI+ mast cells of live CD45+
0.0809
e.
%CD117+ FcεRI+ mast cells of live CD45+
f.
#CD63+ mast cells
g.
%CD63+ mast cells of live CD45+
h.
%CD63+ mast cells of live CD45+
Young
Old
i.
j.
#Adventitial mast cells / mm²
k.
%Activated mast cells
l.
Serum IgE (ng/ml)
m.
Young
Old
CD63 - APC
FSC-A
n.
%CD63+ of mast cells
- DNP
+ DNP
o.
CCL2 (pg/mL)

◂ **Figure 1. Age-induced accumulation of activated mast cells in the atherosclerotic aorta. a.** Experimental set-up: young 10-12 weeks old (light blue bars) and old 75-83 weeks old (dark blue bars) male *Ldlr*$^{-/-}$ mice were fed a chow diet (white dots) or western type diet (grey dots) for 5 weeks. **b.** Flow cytometry was used to detect the **c.** absolute number and **d.** percentage of mast cells of live CD45^{+} cells in the aortic arch and **e.** the peritoneal cavity. Mast cell activation was investigated by flow cytometric analysis of CD63. **f.** the absolute number of CD63^{+} mast cells in the aortic arch and the percentage of CD63^{+} mast cells within live CD45^{+} leukocytes was quantified in **g.** the aortic arch and **h.** the peritoneal cavity. **i.** Mast cells were stained with a napthol AS-D choloroacetate staining. **j.** The total number of mast cells per mm^{2} and **k.** the percentage of activated mast cells in the aortic root were quantified. **e.** Representative images of flow cytometry analysis of CD117^{+}FcεRI^{+} mast cells in the aortic arch. **l.** Total IgE concentrations were measured in the serum. **m.** Bone-marrow derived mast cells from young and old *Ldlr*$^{-/-}$ mice were stimulated *in vitro* stimulation with anti-IgE DNP and analyzed with flow cytometry. **n.** Activation was quantified by means of CD63 expression on live CD117^{+}FcεRI^{+} mast cells. **o.** CCL2 secretion by stimulated mast cells was detected with legendplex analysis. All representative pictures are taken at optical magnification 5x (top) and 20x (bottom); the bar indicates 250 μm (top) and 100 μm (bottom); asterix indicates activated mast cell. n = 7-8 per group for flow cytometry analysis, n=12 per group for histological analysis and n=3 per group for *in vitro* assays. Data represent mean ± SEM.

The age-associated mast cell phenotype is lost in a young atherosclerotic micro-environment

Next, we aimed to examine if the age-related intrinsic changes of mast cells impact atherosclerosis progression or whether the aged micro-environment drives this proatherogenic phenotype. Therefore, we adoptively transferred BMMCs derived from young versus aged *Ldlr*$^{-/-}$ mice into young mast cell deficient *apoE*$^{-/-}$*Kit*$^{W\text{-}sh/W\text{-}sh}$ mice (**Fig. 3a**). Both young (MC_Y) and aged (MC_O) mast cells were detected in similar levels in the peritoneal cavity of the acceptor mice (**Fig. 3b**), demonstrating equal repopulation efficiency. No differences were observed in the percentage of CD63^{+} and of MHC-II^{+} peritoneal mast cells between the groups (**Fig. 3c, d**), already indicating that the age-associated mast cell phenotype as described above is lost in a young micro-environment. As aged activated mast cells *in vitro* secreted more CCL2, a chemokine involved in monocyte recruitment towards the atherosclerotic plaque[22], the percentage of CD11b^{+}F4/80^{+} macrophages was measured in the peritoneal cavity, which were similar between both groups (**Fig. 3e**). Also, the percentage of CD4^{+} T cells did not differ in both the peritoneum and the aortic arch, neither did the percentage of Ki67 expression on these CD4^{+} T cells, indicating that T cell proliferation was not affected (**Fig. 3f-i**). Finally, no differences in atherosclerotic plaque size (**Fig. 3j, k**), percentage vessel occlusion (**Fig. 3j, l**), collagen content (**Fig. 3m, n**) and necrotic core size (**Fig. 3m, o**) were observed. Together, these data indicate that the intrinsic phenotypic changes observed *in vitro*, do not maintain in a long-term *in vivo* setting and that the continued exposure to the aging microenvironment controls mast cell phenotype in atherosclerosis.

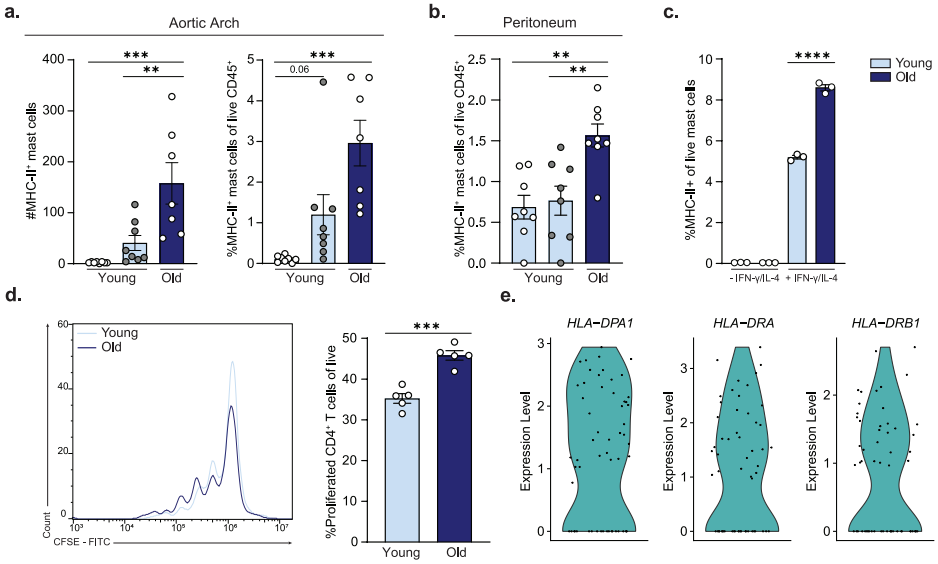

Figure 2. MHCII⁺ expression on aged mast cells induces increased CD4⁺ T cell proliferation. Flow cytometry was used to detect the **a.** absolute number and percentage of MHC-II mast cells of live CD45⁺ cells in the aortic arch and **b.** the peritoneal cavity. **c.** *In vitro* stimulation of young and old bone-marrow derived mast cells with IFN-γ and IL-4 induced MHC-II expression as measured and quantified by flow cytometry. **d.** To assess antigen presenting capacities of young and old bone-marrow derived mast cells, a co-culture was performed of IFN-γ and IL-4 stimulated mast cells with αCD3/αCD28-stimulated OT-II T cells with ovalbumin for 3 days. CD4⁺ T cell proliferation was measured by CFSE staining using flow cytometry. Proliferation was quantified as the percentage of CFSE⁻ CD4⁺ T cells of live cells. **e.** Single-cell RNA sequencing data of human carotid atherosclerotic plaques of 43 patients revealed expression of human MHC-II orthologs *HLA-DPA1*, *HLA-DRA* and *HLA-DRB1* in the mast cell cluster. n = 7-8 per group for flow cytometry analysis and n = 3-5 per group for *in vitro* assays. Data represent mean ± SEM.

Mast cell stabilization reduces the percentage of systemic effector T cells in aged mice

Based on these and our previous findings[21], we hypothesized that mast cells contribute to the local inflammatory environment in the plaque. To specifically address whether the aged mast cell impacts inflammation in the atherosclerotic plaque, we treated aged *Ldlr*$^{-/-}$ mice with a common mast cell stabilizer DSCG (**Fig. 4a**). DSCG treatment did not affect the percentage of mast cells in the aorta or the peritoneal cavity (**Fig. 4b, c; Supplemental Fig. 3b,c**), but did result in a 46% reduction in CD63 expression on peritoneal mast cells (Control: 32.4±4.6% vs. DSCG: 17.5±4.2%, $p<0.05$; **Fig. 4d**). Although the percentage CD63⁺ of mast cells was not affected in the atherosclerotic aorta (**Supplemental Fig. 3a**), a trend towards a decrease in the gMFI of CD63 within aortic mast cells was observed, suggesting that DSCG did affect the activation state of mast cells at the site of disease (**Fig. 4e**).

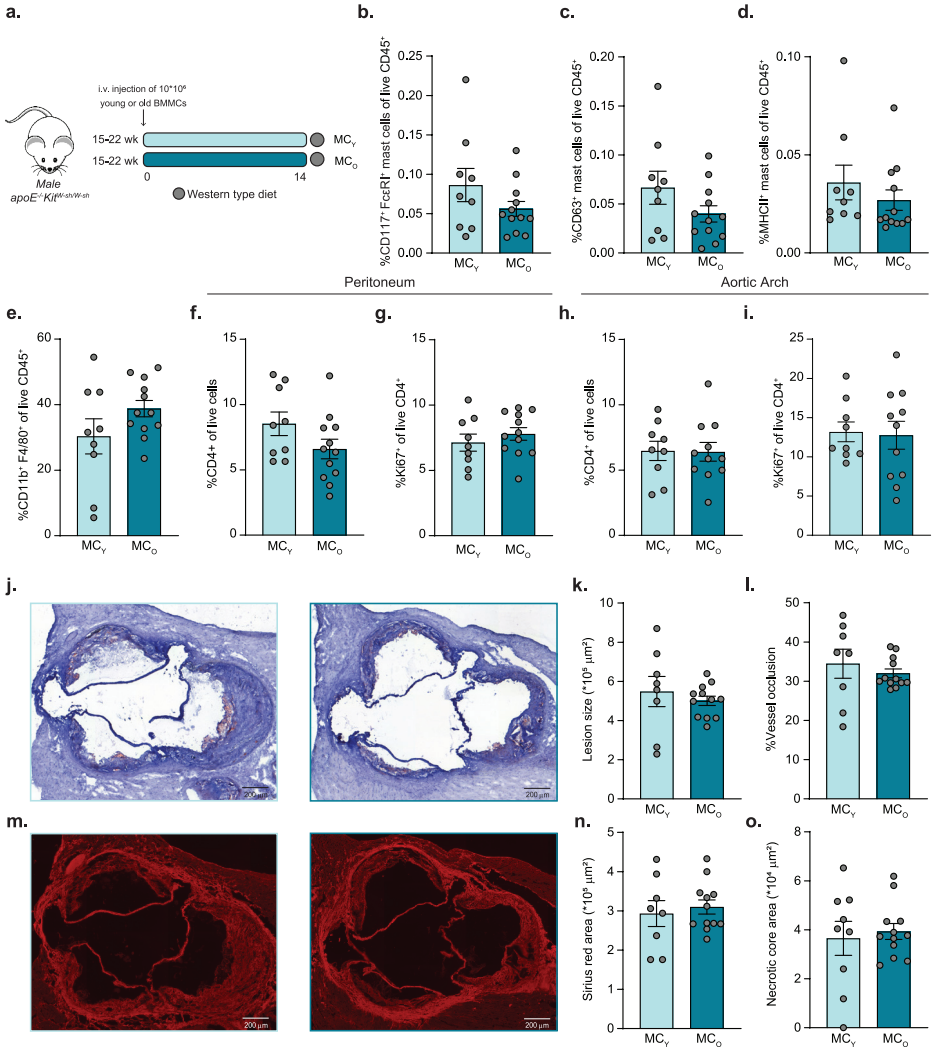
a.
b.
c.
d.
i.v. injection of 10*10⁶ young or old BMMCs
15-22 wk
15-22 wk
MCY
MCO
0
14
Western type diet
Male
apoE-/- KitW-sh/W-sh
%CD117+ FcεRI+ mast cells of live CD45+
%CD63+ mast cells of live CD45+
%MHCII+ mast cells of live CD45+
Peritoneum
Aortic Arch
e.
f.
g.
h.
i.
%CD11b+ F4/80+ of live CD45+
%CD4+ of live cells
%Ki67+ of live CD4+
%CD4+ of live cells
%Ki67+ of live CD4+
j.
k.
l.
m.
n.
o.
Lesion size (*10³ µm²)
%Vessel occlusion
Sirius red area (*10³ µm²)
Necrotic core area (*10⁴ µm²)
200 µm

◂ **Figure 3. Adoptive transfer of young and old mast cells does not alter atherosclerosis progression. a.** Experimental set up: $10*10^6$ young (MC_Y) and old (MC_O) bone marrow-derived mast cells were injected into young mast cell deficient *apoE*$^{-/-}$*Kit*$^{W\text{-}sh/W\text{-}sh}$ mice and simultaneously a western type diet (grey dots) was started for 14 weeks until sacrifice. **b.** Using flow cytometry, reconstitution of mast cells was assessed by measuring CD117$^+$FcεRI$^+$ mast cells of live cells in the peritoneum. **c.** Activation by means of the percentage of CD63$^+$ mast cells of live CD45$^+$ and **d.** antigen presenting capacities by means of the percentage of MHC-II$^+$ mast cells of live CD45$^+$ was quantified in the peritoneum by flow cytometry. **e.** The percentage of CD11b$^+$F4/80$^+$ peritoneal macrophages of live CD45$^+$ was quantified. Subsequently, the percentage of total CD4$^+$ and proliferating Ki67$^+$CD4$^+$ was measured by flow cytometry in respectively the peritoneum (**f., g.**) and the aortic arch (**h., i.**). **j.** Atherosclerotic plaques in the aortic root were stained by Oil Red O staining to measure **k.** lesion size in μm^2 and **l.** the percentage of vessel occlusion. **m.** Atherosclerotic plaque stability was examined by Sirius Red staining of the aortic root to identify the **n.** Sirius red stained collagen area in μm^2 and **o.** the necrotic core area in μm^2. All representative pictures are taken at optical magnification 5x; the bar indicates 200 μm. n = 9-12 per group. Data represent mean ± SEM.

Subsequently, we investigated whether this mast cell stabilization affected the systemic and local CD4$^+$ T cell content. No difference was detected in the total percentage of CD4$^+$ T cells in (**Supplemental Fig. 3b-d**), the percentage of proliferating CD4$^+$ T cells and the percentage of central memory CD4$^+$ T cells (CD44$^+$CD62L$^+$, **Fig. 5a, b**) in the organs analysed. However, a reduction was observed in circulating and splenic effector CD4$^+$ T cells with DSCG treatment (CD44$^+$CD62L$^+$, Blood: Control: 51.1±2.9% vs. DSCG: 39.5±2.5%, $p<0.05$; Spleen: Control: 58.0±3.0 vs. DSCG: 46.9±2.6%, $p<0.05$; **Fig. 5c**). Moreover, a trend towards a decrease was observed for regulatory T cells in both the spleen and the aortic arch (**Fig. 5d**). In the spleen, Th1 cells were also significantly lower in the DSCG treated group versus control (Control: 23.0±1.0 vs. DSCG: 17.7±1.4, $p<0.05$; **Fig. 5e**). No difference was observed in the percentage of MHCII$^+$ mast cells in respectively the peritoneum and the aortic arch with DSCG treatment (**Fig. 5f, g**). This suggests that the differences in CD4$^+$ T cell phenotype are not due to changes in direct antigen-presentation, but could be mediated by the pro-inflammatory mediators secreted by mast cells. While a 6-weeks DSCG treatment in aged *Ldlr*$^{-/-}$ mice was effective in reducing atherogenic CD4$^+$ T cell content, this did not translate into effects on the aged atherosclerotic plaque size (**Fig. 5h, i**), or morphology as measured by collagen and necrotic core content in this time-frame (**Fig. 5h-k**).

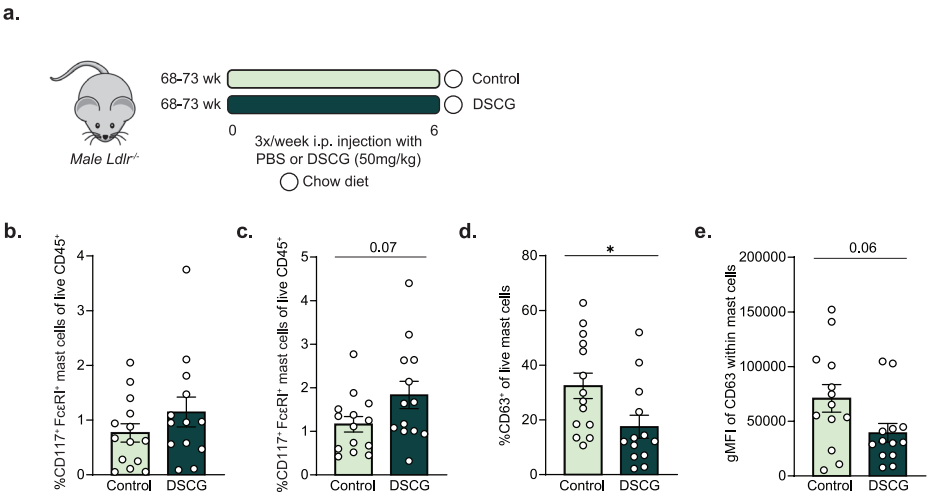

Figure 4. Treatment with DSCG reduces mast cell activation in aged mice. a. Experimental set-up: aged 68-73 weeks old mice were treated with DSCG (50mg/kg) of PBS control three times a week for six weeks. Mice were fed a chow diet (white dots) until sacrifice. Flow cytometry analysis was performed to examine the percentage of mast cells of live CD45$^+$ in **b.** the peritoneum and **c.** the aortic arch. Subsequently DSCG efficacy was examined by measuring **d.** the percentage of CD63$^+$ mast cells of live CD45$^+$ in the peritoneum and **e.** the geometric mean fluorescent intensity of CD63 on mast cells in the aortic arch. n = 13-14 per group. Data represent mean ± SEM.

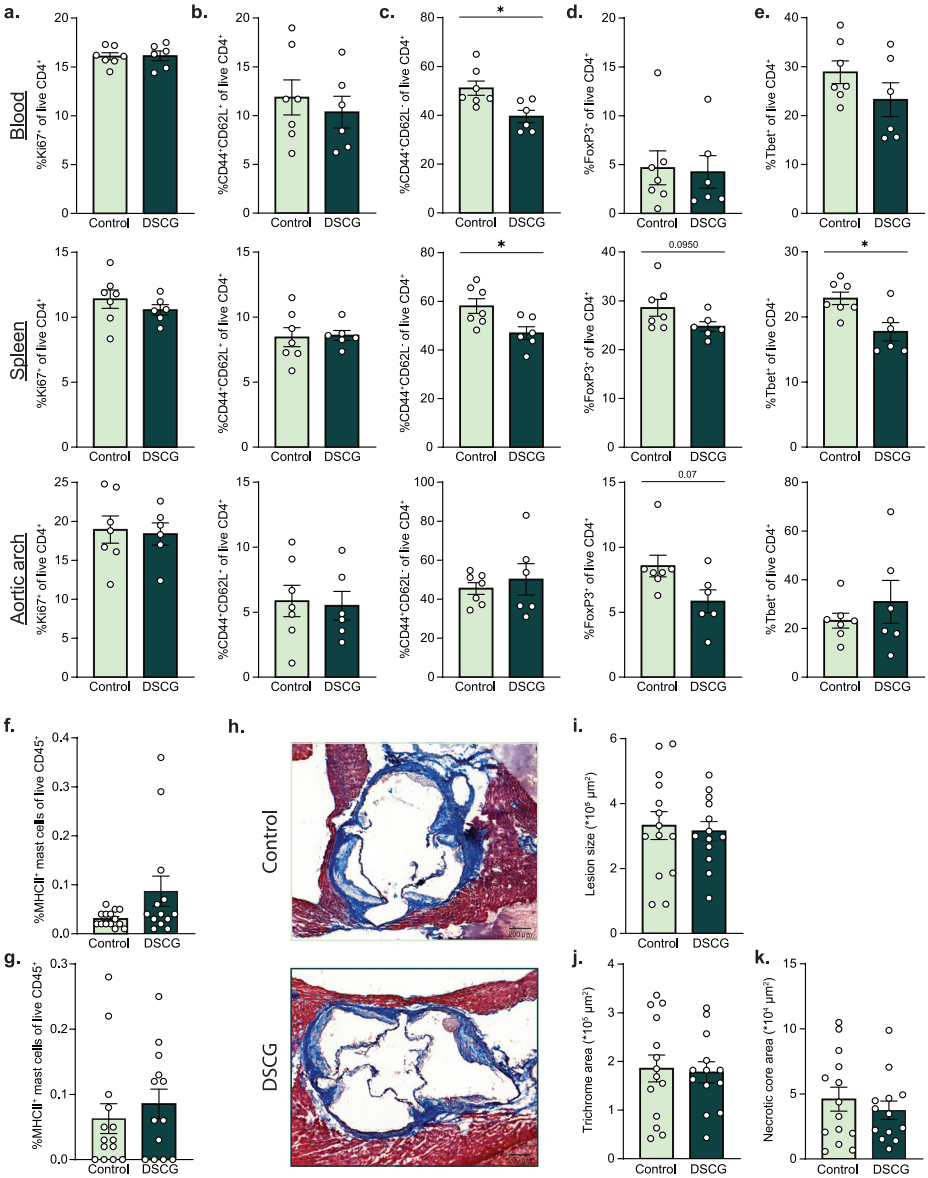
a.
b.
c.
d.
e.
Blood
Spleen
Aortic arch
%Ki67+ of live CD4+
%CD44+CD62L- of live CD4+
%FoxP3+ of live CD4+
%Tbet+ of live CD4+
Control
DSCG
*
0.0950
0.07
f.
g.
h.
i.
j.
k.
%MHCII+ mast cells of live CD45+
Control
DSCG
Lesion size (*10⁶ µm²)
Trichrome area (*10⁵ µm²)
Necrotic core area (*10⁴ µm²)

◂ **Figure 5. Treatment with DSCG reduces effector CD4⁺ T cells but not atherosclerotic plaque size.** Flow cytometry analysis was performed on the blood, spleen and aortic arch to identify respectively the percentage of **a.** Ki67⁺, **b.** CD44⁺CD62L⁺, **c.** CD44⁺CD62L⁻, **d.** Foxp3⁺ and **e.** Tbet⁺ of live CD4⁺ (all vertical). The percentage of MHC-II⁺ mast cells of live CD45⁺ was identified in **f.** the peritoneum and **g.** the aortic arch. **h.** Atherosclerotic plaques in the aortic root were stained by Masson's Trichrome to measure **i.** lesion size in μm^2 and to examine plaque stability by measuring the **j.** trichrome stained collagen area in μm^2 and **k.** the necrotic core area in μm^2. All representative pictures are taken at optical magnification 5x; the bar indicates 200 μm. n = 6-7 per group for flow cytometry analysis and n = 13-14 per group for histological analysis. Data represent mean ± SEM.

Discussion

Aging is a prominent risk factor for the development of atherosclerosis amongst others due to the inflammaging-related proinflammatory environment it induces. Previously, age-associated changes in intraplaque immune cells have been described[16], yet whether age also affects mast cells remained elusive. In this study, we therefore aimed to examine age-induced phenotypic changes of mast cells in atherosclerosis. Here we show that the aged microenvironment promotes local accumulation of mast cells and its activation which subsequently affects local and systemic CD4⁺ T cell proliferation and phenotype.

Interestingly, mast cell accumulation has previously been reported to associate with aging and age-related disease. Increased mast cell numbers were detected in the aged skin[11,14], gut and brain[10], as well as the brain of Parkinson's disease patients.[23,24] Additionally, gut mast cell numbers further expanded after middle cerebral artery occlusion, which mimics stroke. In line, we describe an increase in the proportion of mast cells in the peritoneum and atherosclerotic aortic arch upon aging.

Besides increased numbers of mast cells in aged atherosclerosis, our data also show that they exert a predominantly activated phenotype both in the peritoneum and the atherosclerotic aortic arch. The effects of age on mast cell activation and degranulation are to date still rather contradictory and differ per tissue. Whereas mast cells surrounding the mesenteric lymphatic vessels showed a 400% increase in activation in resting mesenterium of aged mice, less degranulation was observed in the papillary dermis of old individuals.[11,15] Nevertheless, in cardiovascular disease serum tryptase levels have been found twice as high in patients with acute myocardial infarction versus unsubstantial coronary heart disease patients.[25] Furthermore, a significant correlation has been found between serum tryptase level and age in these patients. Congruently, when comparing patients with ST Segment Elevation Myocardial

Infarction (STEMI) with healthy controls a similar increase in serum tryptase was detected as well as a positive correlation with age.[26] Moreover, in human carotid atherosclerotic plaques, the vast majority of detected mast cells were positive for CD63.[27] These data further support the hypothesis that mast cells have an increased activated phenotype in aged cardiovascular disease patients. A possible explanation for the activated mast cell phenotype in atherosclerosis could be an increase in activation via the IgE-FcεR-pathway. Serum IgE levels are generally described to be associated to cardiovascular disease and[28] we previously found the majority of the activated human intraplaque mast cells to have IgE bound to the surface. In addition, elevated levels of IgE sensitive to α-Gal were positively correlated with increased atheroma burden and an unstable plaque phenotype.[27,29] In this study, we observed an elevated serum IgE concentration in aged *Ldlr*$^{-/-}$ mice as well, together suggesting a prominent role for the IgE-FcεRI mediated pathway of activation.

Although we detected intrinsic changes in mast cell activation using BMMCs from aged mice, this did not sustain upon adoptive transfer in young mast cell deficient *apoE*$^{-/-}$*Kit*$^{W\text{-}sh/W\text{-}sh}$ mice. Mast cell phenotype can be altered by the local cytokine content.[30–34] Hereto, the inflammaging could indeed induce phenotypic changes, not only by the pro-inflammatory cytokines, but also due to interactions with neighboring aged immune cells. Indeed, our data emphasize the importance of the aging microenvironment on mast cell phenotype in atherosclerosis.

Recently, a prominent role for CD4$^+$ T cells in atherosclerosis has been proposed by reporting a plaque-specific clonal expansion suggesting that atherosclerosis has autoimmune-like components.[35] These CD4$^+$ T cells can be activated via interaction with classical antigen-presenting cells, including dendritic cells and macrophages. However, mast cells act as atypical antigen-presenting cells as well.[19] Gaudenzio *et al*. showed that in the skin of psoriasis patients, mast cells were observed in close contact with CD4$^+$ T cells.[36] Furthermore, in a murine model of multiple sclerosis, a reduction of CD44 expression as well as reduced T cell infiltration in the central nervous system was observed upon mast cell depletion.[37] In the context of atherosclerosis, previous work of our lab not only showed that hyperlipidemic serum upregulated MHC-II expression on mast cells, but that these mast cells were also capable of antigen presentation *in vivo* and that mast cell deficiency significantly reduced CD4$^+$ T cell proliferation in the atherosclerotic aorta.[21] Since we established an increased number of MHC-II$^+$ mast cells in the aged atherosclerotic aorta, we sought to examine whether this could affect the intraplaque CD4$^+$ T cells as well. Indeed, we observed increased CD4$^+$ T cell proliferation, indicating that the aged MHC-II$^+$ mast cells were capable of direct antigen presentation. Moreover, this *in vitro* assay also presented

evidence that mast cells are able to internalize ovalbumin and present it to $CD4^+$ T cells. This aligns with previous work reporting that mast cells are capable of IFN-γ independent uptake of soluble and particulate antigens.[38] Additionally, they state that mast cell degranulation increases surface delivery of antigen to the MHC-II molecule, further enhancing $CD4^+$ T cell proliferation. *In vivo*, however, upregulation of MHC-II is probably dependent on the aged microenvironment in which the mast cell resides, since with adoptive transfer this phenotype and effect on $CD4^+$ T cell proliferation was lost. Nevertheless, this implies that the expression of human orthologs of MHC-II on human intraplaque mast cells could thus contribute to $CD4^+$ T cell proliferation in the human atherosclerotic lesion of aged CVD patients.

Although direct antigen presentation by mast cells likely occurs in the plaque, we hypothesized that the pro-inflammatory cytokines secreted by activated mast cells could even have more impact on $CD4^+$ T cell proliferation during disease development. Indeed, mast cells have been described to affect T cell migration and polarization by their cytokine secretion upon activation.[39] By using the mast cell stabilizer DSCG as tool to inhibit degranulation, we could subsequently investigate the contribution of the mast cell secretome on $CD4^+$ T cell proliferation and phenotype in aged atherosclerotic mice. Although we did not find differences in $CD4^+$ T cell proliferation, we do report reduced systemic and intraplaque effector $CD4^+$ T cells as a consequence of reduced mast cell activation. Furthermore, particularly $FoxP3^+$ and $Tbet^+$ $CD4^+$ T cells were reduced by mast cell stabilization. Correspondingly, mast cells have been described to play a crucial role in the migration of tolerogenic dendritic cells as well as priming dendritic cells to promote subsequent Th1 and Th17 responses.[39–41] This suggest that the pro-inflammatory cytokines secreted by mast cells indeed affects $CD4^+$ T cell phenotype in atherosclerosis, yet further functional studies will be necessary to confirm this hypothesis.

To conclude, we report an age-induced accumulation of activated mast cells in the atherosclerotic plaque. Moreover, we demonstrate that mast cells contribute to intraplaque $CD4^+$ T cell proliferation and differentiation and emphasize how these changes are dependent on the aged microenvironment. It is thus of great importance to consider age in future research targeting mast cells, and other immune cells, in the development of new treatments for atherosclerosis.

Funding

This work was supported by the Dutch Heart Foundation (grant number 2018T051 to ACF), and the European Research Area Network on Cardiovascular Diseases (ERA-CVD) B-eatATHERO consortium (to ACF). IB is an Established Investigator of the Dutch Heart Foundation (2019T067). M.A.C.D., B.S., J.K., I.B. are supported by the

Dutch Heart Foundation (Generating the best evidence-based pharmaceutical targets and drugs for atherosclerosis (GENIUS II); grant number CVON2017-20). M.A.C.D., I.B., J.K. are supported by the NWO-ZonMW (PTO program grant number 95105013).

Disclosures

The authors have no conflicts of interest to disclose.

References

1. Libby, P. *et al.* Atherosclerosis. *Nature Reviews Disease Primers 2019 5:1* **5**, 1–18 (2019).
2. Krishnaswamy, G., Ajitawi, O. & Chi, D. S. The human mast cell: an overview. *Methods Mol Biol* **315**, 13–34 (2006).
3. Valent, P. *et al.* Mast cells as a unique hematopoietic lineage and cell system: From Paul Ehrlich's visions to precision medicine concepts. *Theranostics* **10**, 10743–10768 (2020).
4. Bot, I. *et al.* Perivascular mast cells promote atherogenesis and induce plaque destabilization in apolipoprotein E-deficient mice. *Circulation* **115**, 2516–2525 (2007).
5. Sun, J. *et al.* Mast cells promote atherosclerosis by releasing proinflammatory cytokines. *Nat Med* **13**, 719–724 (2007).
6. Willems, S. *et al.* Mast cells in human carotid atherosclerotic plaques are associated with intraplaque microvessel density and the occurrence of future cardiovascular events. *Eur Heart J* **34**, 3699–3706 (2013).
7. Niccoli, T. & Partridge, L. Ageing as a risk factor for disease. *Curr Biol* **22**, (2012).
8. Ho, Y. H. *et al.* Remodeling of Bone Marrow Hematopoietic Stem Cell Niches Promotes Myeloid Cell Expansion during Premature or Physiological Aging. *Cell Stem Cell* **25**, 407-418.e6 (2019).
9. Kutukova, N. A., Nazarov, P. G., Kudryavtseva, G. V. & Shishkin, V. I. Mast cells and aging. *Advances in Gerontology* **7**, 68–75 (2017).
10. Blasco, M. P. *et al.* Age-dependent involvement of gut mast cells and histamine in post-stroke inflammation. *J Neuroinflammation* **17**, (2020).
11. Pilkington, S. M., Barron, M. J., Watson, R. E. B., Griffiths, C. E. M. & Bulfone-Paus, S. Aged human skin accumulates mast cells with altered functionality that localize to macrophages and vasoactive intestinal peptide-positive nerve fibres. *Br J Dermatol* **180**, 849–858 (2019).
12. Verhoeven, B. A. N. *et al.* Athero-express: Differential atherosclerotic plaque expression of mRNA and protein in relation to cardiovascular events and patient characteristics. Rationale and design. *Eur J Epidemiol* **19**, 1127–1133 (2004).
13. Depuydt, M. A. C. *et al.* Microanatomy of the Human Atherosclerotic Plaque by Single-Cell Transcriptomics. *Circ Res* **127**, 1437–1455 (2020).
14. Gunin, A. G., Kornilova, N. K., Vasilieva, O. V. & Petrov, V. V. Age-related changes in proliferation, the numbers of mast cells, eosinophils, and cd45-positive cells in human dermis. *J Gerontol A Biol Sci Med Sci* **66**, 385–392 (2011).
15. Chatterjee, V. & Gashev, A. A. Aging-associated shifts in functional status of mast cells located by adult and aged mesenteric lymphatic vessels. *Am J Physiol Heart Circ Physiol* **303**, (2012).
16. Smit, V. *et al.* Single-cell profiling reveals age-associated immunity in atherosclerosis. *Cardiovasc Res* (2023) doi:10.1093/CVR/CVAD099.
17. Orinska, Z., Hagemann, P. M., Halova, I. & Draber, P. Tetraspanins in the regulation of mast cell function. *Med Microbiol Immunol* **209**, 531–543 (2020).
18. Bot, I., Shi, G. P. & Kovanen, P. T. Mast cells as effectors in atherosclerosis. *Arterioscler Thromb Vasc Biol* **35**, 265 (2015).
19. Kambayashi, T. & Laufer, T. M. Atypical MHC class II-expressing antigen-presenting cells: can anything replace a dendritic cell? *Nature Reviews Immunology 2014 14:11* **14**, 719–730 (2014).
20. Gaudenzio, N. *et al.* Cell-cell cooperation at the T helper cell/mast cell immunological synapse. *Blood* **114**, 4979–4988 (2009).

21. Kritikou, E. *et al.* Hypercholesterolemia Induces a Mast Cell-CD4+ T Cell Interaction in Atherosclerosis. *J Immunol* **202**, 1531–1539 (2019).
22. Kim, K. W., Ivanov, S. & Williams, J. W. Monocyte Recruitment, Specification, and Function in Atherosclerosis. *Cells* **10**, (2021).
23. Kempuraj, D. *et al.* Mast Cell Proteases Activate Astrocytes and Glia-Neurons and Release Interleukin-33 by Activating p38 and ERK1/2 MAPKs and NF-κB. *Mol Neurobiol* **56**, 1681–1693 (2019).
24. Zhang, X. *et al.* Immune Profiling of Parkinson's Disease Revealed Its Association With a Subset of Infiltrating Cells and Signature Genes. *Front Aging Neurosci* **13**, (2021).
25. Xiang, M. *et al.* Usefulness of serum tryptase level as an independent biomarker for coronary plaque instability in a Chinese population. *Atherosclerosis* **215**, 494–499 (2011).
26. Lewicki, L. *et al.* Elevated Serum Tryptase and Endothelin in Patients with ST Segment Elevation Myocardial Infarction: Preliminary Report. *Mediators Inflamm* **2015**, (2015).
27. Kritikou, E. *et al.* Flow Cytometry-Based Characterization of Mast Cells in Human Atherosclerosis. *Cells* **8**, (2019).
28. Kounis, N. G. & Hahalis, G. Serum IgE levels in coronary artery disease. *Atherosclerosis* **251**, 498–500 (2016).
29. Wilson, J. M. *et al.* IgE to the Mammalian Oligosaccharide Galactose-α-1,3-Galactose Is Associated With Increased Atheroma Volume and Plaques With Unstable Characteristics-Brief Report. *Arterioscler Thromb Vasc Biol* **38**, 1665–1669 (2018).
30. da Silva, E. Z. M., Jamur, M. C. & Oliver, C. Mast cell function: a new vision of an old cell. *J Histochem Cytochem* **62**, 698–738 (2014).
31. Galli, S. J. *et al.* Mast cells as 'tunable' effector and immunoregulatory cells: recent advances. *Annu Rev Immunol* **23**, 749–786 (2005).
32. Reber, L. L., Sibilano, R., Mukai, K. & Galli, S. J. Potential effector and immunoregulatory functions of mast cells in mucosal immunity. *Mucosal Immunol* **8**, 444–463 (2015).
33. Franceschi, C., Garagnani, P., Parini, P., Giuliani, C. & Santoro, A. Inflammaging: a new immune-metabolic viewpoint for age-related diseases. *Nat Rev Endocrinol* **14**, 576–590 (2018).
34. Tan, Q., Liang, N., Zhang, X. & Li, J. Dynamic Aging: Channeled Through Microenvironment. *Front Physiol* **12**, (2021).
35. Depuydt, M. A. C. *et al.* Single-cell T cell receptor sequencing of paired human atherosclerotic plaques and blood reveals autoimmune-like features of expanded effector T cells. *Nature Cardiovascular Research 2023 2:2* **2**, 112–125 (2023).
36. Gaudenzio, N., Laurent, C., Valitutti, S. & Espinosa, E. Human mast cells drive memory CD4+ T cells toward an inflammatory IL-22+ phenotype. *J Allergy Clin Immunol* **131**, (2013).
37. Gregory, G. D., Robbie-Ryan, M., Secor, V. H., Sabatino, J. J. & Brown, M. A. Mast cells are required for optimal autoreactive T cell responses in a murine model of multiple sclerosis. *Eur J Immunol* **35**, 3478–3486 (2005).
38. Lotfi-Emran, S. *et al.* Human mast cells present antigen to autologous CD4+ T cells. *J Allergy Clin Immunol* **141**, 311-321.e10 (2018).
39. Bulfone-Paus, S. & Bahri, R. Mast Cells as Regulators of T Cell Responses. *Front Immunol* **6**, (2015).
40. de Vries, V. C. *et al.* Mast cells condition dendritic cells to mediate allograft tolerance. *Immunity* **35**, 550–561 (2011).
41. Morita, H., Saito, H., Matsumoto, K. & Nakae, S. Regulatory roles of mast cells in immune responses. *Semin Immunopathol* **38**, 623–629 (2016).

Supplemental Figures

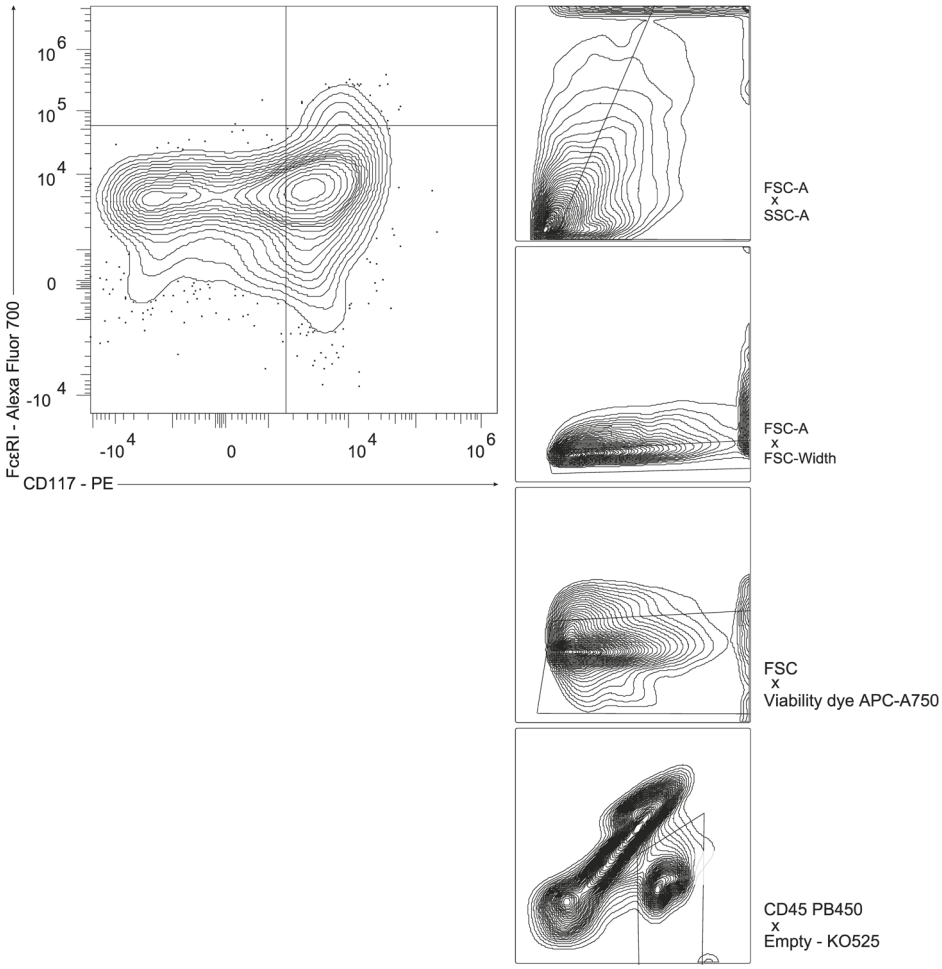

Supplemental figure 1. Gating strategy of mast cells in the aortic arch. First cells were selected (FSC-A x SSC-A), singlets were gated (FSC-A x FSC-W). Subsequently live cells were gated as Viability Dye negative population of singlets. CD45^{+} cells were isolated by gating against an empty channel. Finally CD117^{+}FcεRI^{+} cells were gated as mast cells for the analysis.

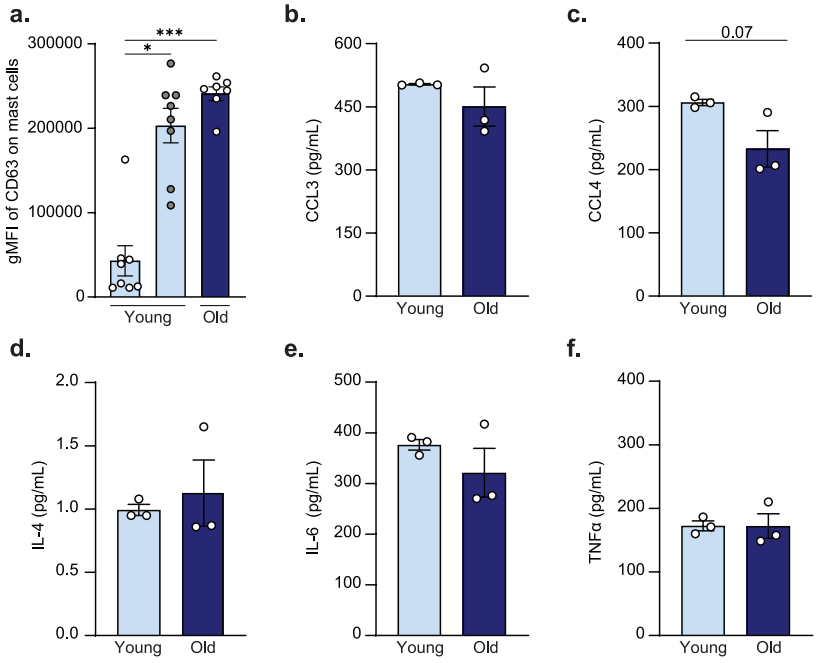

Supplemental figure 2. Increase in gMFI of CD63⁺ on mast cells with both WD and age in the atherosclerotic aorta. a. Flow cytometric analysis of the gMFI of CD63⁺ mast cells of live CD45⁺ in the aortic arch. Legendplex analysis of the supernatant of *in vitro* IgE-DNP stimulated young and old bone marrow-derived mast cells measuring the concentration of **b.** CCL3, **c.** CCL4, **d.** IL-4**, e.** IL-6 and **f.** TNFα in pg/mL. n = 7-8 for flow cytometry data. n = 3 for *in vitro* analysis. Data represent mean ± SEM.

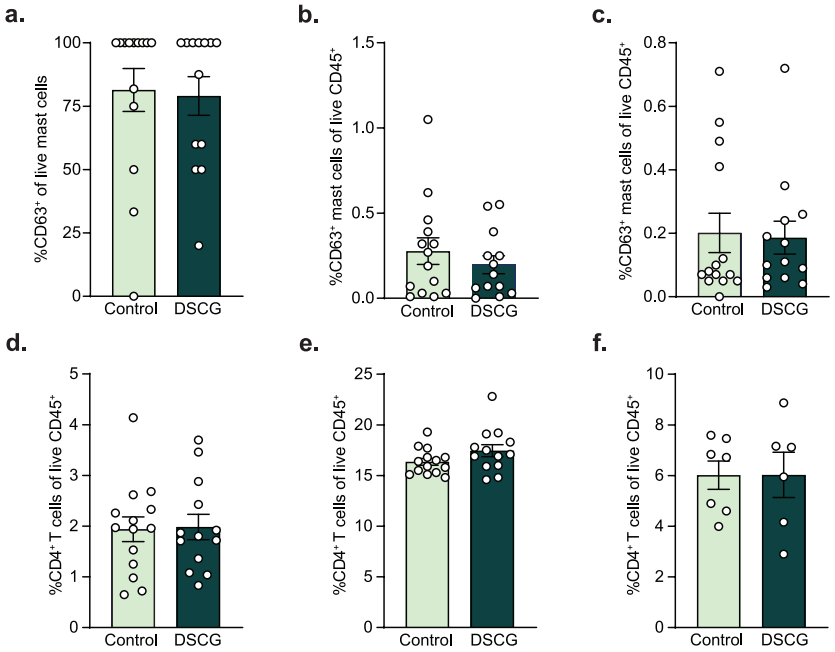

Supplemental figure 3. No difference in the percentage of CD63⁺ mast cells of live CD45⁺ in the peritoneum and aortic arch. a. Flow cytometry analysis of the percentage of CD63⁺ of live mast cells in the aortic arch. No difference was observed in the percentage of CD63⁺ mast cells of live CD45⁺ in both **b.** the peritoneum and **c.** the aortic arch with flow cytometry. Furthermore, the percentage of total CD4⁺ T cells of live CD45⁺ was measured in respectively **d.** the blood, **e.** the spleen and **f.** the aortic arch. n = 13-14 per group for flow cytometry analysis. n = 6-7 per group for CD4⁺ T cell analysis in the aortic arch. Data represent mean ± SEM.